Published in final edited form as:
Eur J Neurosci. 2007 October ; 26(7): 1940–1949.

Evidence for RPE65-independent vision in the cone-dominated zebrafish retina

Helia B. Schonthaler[1,§,*], **Johanna M. Lampert**[2,†,*], **Andrea Isken**[2,*], **Oliver Rinner**[1,‡,*], **Andreas Mader**[2], **Matthias Gesemann**[1], **Vitus Oberhauser**[2], **Marcin Golczak**[3], **Oliver Biehlmaier**[1], **Krzysztof Palczewski**[3], **Stephan C. F. Neuhauss**[1], and **Johannes von Lintig**[2]

[1]*University of Zurich, Institute of Zoology, Winterthurerstrasse 190, CH-8057 Zurich, Switzerland* [2]*Institute of Biology I, University of Freiburg, Hauptstrasse 1, D-79104 Freiburg, Germany* [3]*Department of Pharmacology, School of Medicine, Case Western Reserve University, Cleveland, OH 44106–4965, USA*

Abstract

An enzyme-based cyclic pathway for *trans* to *cis* isomerization of the chromophore of visual pigments (11-*cis*-retinal) is intrinsic to vertebrate cone and rod vision. This process, called the visual cycle, is mostly characterized in rod-dominated retinas and essentially depends on RPE65, an all-*trans* to 11-*cis*-retinoid isomerase. Here we analysed the role of RPE65 in zebrafish, a species with a cone-dominated retina. We cloned zebrafish *RPE65* and showed that its expression coincided with photoreceptor development. Targeted gene knockdown of RPE65 resulted in morphologically altered rod outer segments and overall reduced 11-*cis*-retinal levels. Cone vision of RPE65-deficient larvae remained functional as demonstrated by behavioural tests and by metabolite profiling for retinoids. Furthermore, all-*trans* retinylamine, a potent inhibitor of the rod visual cycle, reduced 11-*cis*-retinal levels of control larvae to a similar extent but showed no additive effects in RPE65-deficient larvae. Thus, our study of zebrafish provides *in vivo* evidence for the existence of an RPE65-independent pathway for the regeneration of 11-*cis*-retinal for cone vision.

Keywords

11-*cis*-retinal; photoreceptor development; pigment epithelium; retinal photoreceptor; retinoids; visual cycle

Introduction

The vertebrate visual system employs two types of photoreceptors working at different light intensities. Rods are specialized for vision under dim light conditions, whereas cones are active under daylight conditions, enabling high-resolution colour vision (Rodieck, 1998). Both rod and cone visual pigments are of bipartite structure, consisting of a transmembrane protein (opsin) and the vitamin A-derived chromophore 11-*cis*-retinal (11-*cis*-RAL; Palczewski, 2006). Light absorption leads to isomerization of the chromophore from the 11-*cis* to the all-*trans* configuration resulting in the metarhodopsin state, which activates a signal transduction cascade (Burns & Baylor, 2001). Finally, the visual pigment decays into the opsin moiety and

Correspondence: Dr Johannes von Lintig or Dr Stephan Neuhauss, as above. E-mail: lintig@biologie.uni-freiburg.de or stephan.neuhauss@zool.uzh.ch.
†Present address: Harvard University, 16 Divinity Avenue, Cambridge, MA 02138, USA.
‡Present address: Swiss Federal Institute of Technology, Hönggerberg HPT E76, CH-8093 Zurich, Switzerland.
§Present address: Research Institute of Molecular Pathology (IMP) A-1030 Vienna, Austria.
*H.B.S., J.M.L., A.I. and O.R. contributed equally to this study.

all-*trans*-RAL, which must be recycled to 11-*cis*-RAL to support continuous vision (McBee *et al*., 2001; Lamb & Pugh, 2004).

Detailed knowledge about this process, called the visual (retinoid) cycle (Wald, 1968), stems from work on species with rod-dominated retinas such as mice. Here, the visual cycle (for rods) involves two cellular compartments, the rod outer segments (ROS) and the closely associated retinal pigment epithelium (RPE). The re-isomerization to the 11-*cis* conformation of the visual chromophore is achieved by a two-step enzymatic reaction in the RPE (Bernstein *et al*., 1987; Rando, 1991). Thereby, the action of lecithin retinol acyltransferase (LRAT) on all-*trans*-retinol (ROL) generates retinyl esters (RE), which are further processed into 11-*cis*-ROL by an isomerase. The latter enzyme was recently identified as retinal pigment epithelium-specific 65-kDa protein (RPE65), an abundant protein in the RPE (Jin *et al*., 2005; Moiseyev *et al*., 2005; Redmond *et al.*, 2005).

Cones are operative under bright light, under which rods are saturated but consume 11-*cis*-RAL. This condition might necessitate a cone-specific regeneration pathway to avoid competition for 11-*cis*-RAL between the two types of photoreceptors. In mice, a *RPE65*-null mutation results in 11-*cis*-RAL deficiency and results in severely impaired cone and rod function (Seeliger *et al*., 2001). In contrast, in cone-dominated animals such as chicken, evidence has been provided for an additional cone-specific pathway for the recycling of the visual chromophore. Recent biochemical studies showed that this pathway probably takes place in cone photoreceptors and Müller glia cells (Mata *et al*., 2002) and thus is probably RPE65-independent.

In vivo investigations on the role of RPE65 in cone-dominated animals have been hampered by a lack of a suitable model organism. In this study, we used the larva of the zebrafish (*Danio rerio*), which is excellently suited for genetic and pharmacological manipulations. Even though cone and rod photoreceptors develop concomitantly (Schmitt & Dowling, 1996), the retina is functionally cone-dominated at early larval stages (Bilotta *et al*., 2001). We cloned gene orthologues for *RPE65* and showed that one of these is expressed in the RPE of the larval eyes. We then disrupted the RPE65-dependent visual cycle by genetic and pharmacological manipulation by morpholino (MO) oligonucleotides (Nasevicius & Ekker, 2000) and all-*trans* retinyl amine (Ret-NH_2; Golczak *et al*., 2005b). Targeted gene knockdown of RPE65 resulted in morphologically altered ROSs and overall reduced 11-*cis*-RAL levels. Ret-NH_2, a potent inhibitor of RPE65 enzymatic activity, reduced 11-*cis*-RAL levels to a similar extent but showed no additive effects in RPE65-deficient larvae. Under all conditions, the residual 11-*cis*-RAL was efficiently regenerated and cones remained functional as demonstrated by behavioural tests.

Materials and methods

Fish maintenance and strains

Zebrafish were bred and maintained under standard conditions at 28 °C (Westerfield, 1994). Embryos from the AB/TL strain were used for the expression analyses. Morphological features characteristic of developmental stages were used to determine the stage of the embryos in hours post-fertilization (hpf), according to (Kimmel *et al*., 1995). Embryos used for *in situ* hybridization experiments were raised in the presence of 200 μM 1-phenyl-2-thiourea (Sigma) to inhibit pigmentation. Embryos were anaesthesized with 0.2% Tricaine solution (Sigma) before fixation. Adult fish for eye extirpation were deeply anaesthesized with Tricaine solution on ice. All animal procedures were approved by local animal welfare authorities, according to German and Swiss law.

Cloning of RPE65a and RPE65b

Total RNA was isolated from adult zebrafish eyes by using the RNAeasy Kit (QIAGEN, Germany) according to the manufacturer's instructions. cDNA was synthesized by using the SuperScript II Reverse Transcriptase Kit (Invitrogen, Germany) as described in the user's manual. The *RPE65a* cDNA was cloned by RT-PCR using degenerated primers designed against a 519-bp fragment of cDNA deduced from highly conserved amino acid sequences: TGGGGAGCNAAYTAYATGGA, GGYTCYTGCCANAYCCA. The PCR product was cloned into SK-pBluescript (Invitrogen) and sequenced with T7 and T3 primers. Additionally, a zebrafish cDNA clone (GenBank accession no. AI942672, AI884144) encoding a putative *RPE65* gene was identified by searching the expressed sequencing tag (EST) database. The clone was obtained from the RZPD (Resource Center/Primary Database, Germany), regrown and purified. Finally, the clone was sequenced with M13 reverse primer and M13 (−20) forward primer, and the full length of the clone was obtained by sequencing using gene-specific primers: AGGTTTTTCACTTACTTTCAAGG, CCACATTAACTGTTTTGAAGACC, ACTTCCTGGAGCATCAGAGG and AGGACGTCAACCTCCGCACG. The sequencing of the EST resulted in a second *RPE65* cDNA, named *RPE65b*. To obtain the 5′- and 3′-cDNA sequences of the two genes, RACE-PCRs were carried out with the SMART RACE cDNA Amplification Kit (Clontech, Germany). The RACE primers used to amplify the 5′ primer region of *RPE65a* were GCTGAAGTTTCTGAGCGCCTGGAGCA and for the nested PCR GCCATCCTACGTGCACAGTTTTGGGA. The primers used to amplify the 3′ primer region of *RPE65a* were TGCTCCAGGCGCTCAGAAACTTCAGC and TCCCAAAACTGTGCACGTAGGATGGC. To obtain the 5′ primer region of *RPE65b* nested PCR was also carried out using the following primers: AACCGACAGATAATTGCAGAGGTCCACC and for the nested PCR GTTTCCAGGGTATCAGGATTGACTTTGG. The fragments obtained were then cloned into the pCR2.1 vector (Clontech) and pCRII-TOPO vector (Invitrogen), respectively. The constructs were sequenced using M13 reverse primer and M13 (−20) forward primer. Accession Numbers (GenBank) were as follows: zebrafish RPE65a, AY646886; zebrafish RPE65b, AY646887.

Whole-mount *in situ* hybridization and immunostaining

Whole-mount *in situ* hybridization was performed as previously described (Hauptmann & Gerster, 1994), using RPE65a, RPE65b and rhodopsin as probes. Rhodopsin antisense RNA probe used for *in situ* hybridization was a gift from Dr Wolfgang Driever (University of Freiburg, Germany). Whole-mount antibody labelling was performed according to Solnica-Krezel & Driever (1994), except that the methanol fixation step was omitted. For RPE65 staining, an antiserum raised against recombinant zebrafish RPE65a was used in a dilution of 1 : 300. For this purpose, recombinant zebrafish RPE65a was purified upon heterologous expression in *E. coli*. One milligram of purified RPE65a protein was used to raise a polyclonal antiserum in rabbits (Eurogentec, Brussels, Belgium). For secondary-antibody staining, Cy3 goat antirabbit IgG (Sigma, Germany; 1 : 500) was used.

Immunohistochemistry

Fixed larvae were cryoprotected in 30% sucrose overnight. Entire larvae were embedded in cryomatrix (Jung; tissue-freezing medium), and rapidly frozen in liquid N_2; 20-μm-thick sections were cut at −20 °C, mounted on superfrost slides and air dried at 37 °C for 2 h. The slides were stored at −20 °C until further use. For immunohistochemistry, slides were thawed, washed three times in phosphate-buffered saline (PBS; 50 mM), pH 7.4, and incubated in 20% NGS and 2% BSA in 0.3% Triton X-100 in PBS for 1 h. For double cone and rod labelling, sections were incubated with antimouse zpr1 (1 : 20; Zebrafish International Resource Center, Eugene, USA) and 1D1 (1 : 100; kindly provided by Drs Ann Morris and Jim Fadool, Florida

State University, Tallahassee, USA). The immunoreaction was visualized by using Alexa Fluor 488 antimouse IgG (1 : 1000; Molecular Probes, Leiden, Netherlands) as a secondary antibody. For all immunocytochemical experiments, negative controls were carried out in the same way but without using the first antibody. Slides were viewed with an Olympus BX61 compound microscope (Olympus, Hamburg, Germany). The obtained images were processed using Adobe Photoshop 8.0 (Adobe Systems, San Jose, CA, USA).

Immunoblotting

Immunoblot analysis was performed with zebrafish protein extracts using polyclonal serum raised against murine RPE65 (Wenzel *et al*., 2005) at a 1 : 300 dilution. This antiserum detected both recombinant RPE65a and RPE65b produced in *E. coli* (data not shown). As loading control, antiserum raised against beta-tubulin (Chemicon) was used. Immunoblots were developed with the ECL system (Pharmacia, Germany). Quantification was performed by the Quantity-one (version 4.6) software (Biorad, Germany).

Morpholino injections

RPE65 antisense MO 5′-CAGGGTGTTCAAAACGGCTGACCAT-3′ (GeneTools, LLC) in 0.3 × Danieau's solution (1 × Danieau, in mM: NaCl, 58; KCl, 0.7; $MgSO_4$, 0.4; $Ca(NO_3)_2$, 0.6; and Hepes, 5; pH 7.6) to obtain a stock concentration of 1 mM. Embryos were injected at the one-cell stage at ~8 ng per zygote. Control MOs from GeneTools were injected with the same concentration.

Light treatments of zebrafish larvae

For all illumination experiments, we used a KL 1500-T electronic fibre optic device (Schott, Germany). Before illumination (10 000 lux, bright white light), zebrafish larvae were placed into Petri dishes under dim red light. The bottom and the sides of these dishes were coated with light-reflecting aluminium foil. Upon the different illumination regimens, larvae were immediately collected, killed on ice and stored at −70 °C prior to high-performance liquid chromatography (HPLC) analysis.

Expressing of RPE65 and LRAT in Sf9 cells and isomerization assay

Human RPE65 and mouse LRAT cDNA was cloned into pFastBac HT B vector (Invitrogen) using EheI, HindIII and BamH1, HindIII restriction sites, respectively. The Bac-to-Bac baculovirus expression system (Invitrogen) was employed to generate recombinant bacmids and produce high-titre baculoviruses stocks. Sf9 cells were cotransfected with P2 stock of baculoviruses encoding RPE65 and LRAT. Two days postinfection, expression of recombinant proteins was verified by immunoblotting using antihuman REP65 antibodies (Novus) and antimouse LRAT antibodies (Moise *et al*., 2007). For the *in vivo* isomerization assays, cells were grown to confluence in six-well plates and infected 48 h prior to the experiment. The medium was replaced with a fresh one containing 5% FBS and 10 μM of all-*trans*-ROL. To prevent inhibition the medium was supplemented with Ret-NH_2 at a final concentration of 3 μM. Cells were incubated in the dark for 18 h, harvested with the medium, mixed with 2 mL of methanol and extracted with 4 mL of hexane. The organic fraction was dried down in a speed-vac, redissolved in 250 μL of hexane and analysed on a normal-phase HPLC (Hewlett Packard 1100) equipped with a diode array detector and an Agilent-Si column (4.6 × 250 mm, 5 μm). Retinoids were separated in 10% ethylacetate in hexane at a flow rate 1.4 mL/min.

Ret-NH_2 synthesis and treatments

Ret-NH_2 was synthesized by reacting all-*trans*-RAL with ammonia under anhydrous conditions followed by reduction with an excess of sodium borohydride as described elsewhere (Golczak *et al*., 2005b). Ret-NH_2 was purified by flash liquid chromatography on silica gel

and the purity of Ret-NH_2 was confirmed by normal- and reverse-phase HPLC analysis. Prior to the experiments, Ret-NH_2 was dissolved in ethanol and added to the egg-water of 5-days post-fertilization (dpf) larvae to obtain final concentrations as indicated in the Results section. Upon 30 min of incubation under dim red light, larvae were subjected to illumination by bright light (10 000 lux for 20 min) and dark-readapted for 45 min prior to HPLC analysis.

Behavioural assays

Visual behaviour was assayed as described in Rinner *et al*. (2005b).

HPLC separation for retinoids

For retinoid analysis, larvae were immediately transferred to ice water after light treatment. Retinoids were extracted under monochromatic light (695 nm) from the anterior of the heads and subjected to HPLC separation as previously described (Lampert *et al*., 2003). For quantification of the molar amounts of retinoids, peak integrals were scaled with defined amounts of reference substances from Sigma- Aldrich (Germany) and were quantified using the 32 Karat software (Beckman Instruments). Student's *t*-test was used for statistical analysis.

Results

RPE65 orthologous genes are expressed in the developing eyes and the pineal gland

With its genetic accessibility and its early-maturing visual system the zebrafish larva presents a unique model for analysing cone vision. To exploit this, we cloned two *RPE65* genes, which we denoted *RPE65a* and *RPE65b*. The deduced proteins are highly homologous with human RPE65, showing 74 and 75%, respectively, amino acid sequence identity. As revealed by RNA *in situ* hybridization, only *RPE65a* was expressed in light-sensitive structures during zebrafish development (Fig. 1A–C). The *RPE65a* transcript was already expressed at 16 hpf in the pineal gland, a light-sensitive endocrine organ (Fig. 1A). Expression in the RPE was initiated in the ventronasal patch at 40 hpf, preceding photoreceptor differentiation by a few hours (Fig. 1B). During subsequent development, expression in the RPE became stronger and more widespread, covering the entire RPE except for the cilliary margin by 56 hpf (Fig. 1C). In crosssections it became clear that retinal *RPE65a* expression was confined to RPE cells (Fig. 1D). By contrast, *RPE65b* mRNA was detectable in migrating neural crest cells during somitogenesis (Fig. 1E). At early larval stages, *RPE65b* mRNA expression was visible in the ventricular zone, the upper and lower jaw and the developing pectoral fins. At later larval stages, RPE65b mRNA expression faded out (Fig. 1H).

Generation of RPE65-deficient zebrafish larvae

In order to address the role of RPE65 for cone vision, we performed a loss-of-function study using a MO-based approach (Nasevicius & Ekker, 2000). This technique is routinely used for embryonic stages but has also been successfully applied to achieve gene knockdown at early larval stages (Rinner *et al*., 2005a; Seiler *et al*., 2005). We designed a MO which specifically blocked the initiation of translation of RPE65a in a coupled *in vitro* transcription–translation system (data not shown). We then injected this MO into eggs of the one-cell stage embryo and determined RPE65 protein levels in the heads of 4 and 5 dpf larvae. We used an antiserum, which detected recombinant RPE65a and RPE65b, to determine RPE65 protein levels by immunoblot analysis. We quantified RPE65 protein levels by densitometry and normalized it to the beta-tubulin loading control. In morphants, we found a reduction by at least 97% (4 dpf) and 88% (5 dpf) of the RPE65 protein levels of controls (Fig. 2A and B). Similar results were obtained in three independent experiments. Additionally, we confirmed RPE65 deficiency in the eyes of 5-dpf morphant larvae by whole-mount immunohistochemistry ($n = 20$; Fig. 2C and D).

Analyses of the eyes of RPE65-deficient larvae

To address the consequences of RPE65 deficiency for the larval eyes, we examined standard histological sections. We found a normal lamination of the distinct retinal layers (Fig. 3A and B). *In situ* hybridization for rhodopsin mRNA showed that its expression pattern was similar in morphants and controls, with the most abundant staining of the dorsal and ventral parts of the retina (Fig. 3C and D). We then performed immunostainings against double cones (zpr1 staining) and rods (1D1 staining) to determine whether the distribution and/or morphology of the photoreceptors was affected in RPE65-deficient animals (n = 5; Fig. 4). Double cone distribution and morphology was identical in the control and MO-treated larvae (Fig. 4A and C). However, even though the distribution of the rods throughout the retina remained unaffected in the morphants, with numerous labelled cells in the ventral and dorsal retina and only few labelled cells in the central part of the retina, the morphology of the photoreceptors was altered (Fig. 4B and D). In a close-up of the dorsal retina, the photoreceptors of control larvae showed the characteristic morphology with rod spherules as well as healthy outer segments (Fig. 4B′). In contrast, RPE65-deficient larvae showed deteriorating rod outer segments that had broken up into several small particles, presumptive phagosomes (Fig. 4D′). Thus, rod photoreceptor function is probably impaired in RPE65a-deficient larvae.

Regeneration of 11-cis-RAL took place in RPE65-deficient larvae

In order to assess the effect of RPE65 deficiency on ocular retinoid metabolism, we performed HPLC analyses. To approach this issue, morphants and control siblings were raised under a standard day : night light regime (14 : 10 h). These larvae were then dark-adapted overnight, divided into three groups (n = 50 per group) and subjected to different illumination regimes. In the first group, retinoid analysis was immediately performed. The second group was bleached by exposure to bright light (10 000 lux) for 20 min. The third group was first bleached and then dark-readapted for 45 min prior to HPLC analysis.

The levels of 11-*cis*-RAL were significantly reduced in dark-adapted RPE65-deficient larvae, consistent with morphological alterations in ROS. In both morphants and controls, the amounts of 11-*cis*-RAL decreased upon bleaching with bright light. Surprisingly, dark-readaptation for 45 min resulted in regeneration of 11-*cis*-RAL to the initial amounts found in the nonbleached groups. Thus, despite RPE65-deficiency 11-*cis*-RAL existed and was regenerated after bleaching with bright light in repeated experiments (n = 3).

In the eyes of both morphants and controls, we found high levels of RE (Table 1). RE accumulation has been reported in *RPE65* $^{-/-}$ mice (Redmond *et al*, 1998). As high levels of RE also existed in controls, but also in the eyes of adult zebrafish (Schonthaler *et al*., 2005), we conclude that this characteristic is not related to RPE65 deficiency. Besides these retinoids, we detected in both morphants and controls all-*trans*-RAL and trace amounts of all-*trans*-ROL. However, 9-*cis*-RAL was not detectable in RPE65-deficient larvae, which exists in *RPE65*$^{-/-}$ mice and recombines with opsin to form isorhodopsin in the absence of 11-*cis*-RAL (Fan *et al*., 2003).

Ret-NH_2 had no effects on 11-cis-RAL regeneration in RPE65-deficient larvae

To exclude the possibility that the residual level of RPE65 in morphant larvae might be responsible for 11-*cis*-RAL regeneration, we performed repeated bleaching experiments and again determined 11- *cis*-RAL levels as a measure of the visual pigment content. For this purpose we subjected 5-dpf morphant and control larvae four times to a 20-min bright light illumination (10 000 lux for 20 min), each time followed by a 10-min dark interval. In repeated experiments (n = 3), HPLC analysis revealed that visual pigments were not bleached out as 11-*cis*-RAL still was detectable in both morphant and control larvae in similar amounts as found upon a single 20-min light bleach (see Table 1 and data not shown).

We then took advantage of Ret-NH_2. This compound has been recently shown to act as a potent pharmacological inhibitor of the rod retinoid cycle (Golczak *et al*., 2005b). To demonstrate that Ret- NH_2 directly inhibits RPE65 enzymatic activity, we established a cell culture system. For this purpose, we cotransfected insect *SF9* cells with expression vectors for LRAT and RPE65, and verified protein expression by immunoblot analysis (Fig. 5A). To measure RPE65 enzymatic activity in the presence and absence of Ret-NH_2, we incubated cells with all-*trans*-ROL. Upon incubation with all-*trans*-ROL alone, these cells produced significant amounts of 11-*cis*-ROL (Fig. 5B and C). In contrast, cells incubated with both all-*trans*-ROL and Ret-NH_2 failed to produce 11-*cis*-ROL (Fig. 5B and C). Thus, Ret-NH_2 was able to inhibit RPE65 enzymatic activity.

We then tested the effects of Ret-NH_2 treatment in wild-type larvae. For this purpose, we added Ret-NH_2 (5 μM final concentration) to the water and incubated the larvae for 30 min under dim red light. We then exposed the larvae to bright light illumination (10 000 lux for 20 min) and determined the 11-*cis*-RAL levels upon 45 min dark-readaption. Under this condition, 11-*cis*-RAL levels were significantly reduced as compared to non-treated larvae, but visual pigments were not bleached out (Fig. 6A). No further reduction in 11-*cis*-RAL levels was observed when we doubled the concentration of the inhibitor (data not shown). While 11-*cis*-RAL levels decreased in Ret-NH_2-treated larvae, ROL levels and RE levels increased, most probably due to a deamination of Ret-NH_2 to ROL and subsequent esterification (Golczak *et al*., 2005a). The authenticity of all different retinoid derivatives was verified with authentic standard substances (Fig. 6C). Additionally, N-retinylamides became detectable (Fig. 6B); these are formed by the action of LRAT from Ret-NH_2 (Golczak *et al*., 2005a). Interestingly, Ret-NH_2 treatment caused a similar reduction in 11-*cis*-RAL, ~50% of the levels in control larvae, as we observed upon the targeted gene knockdown of RPE65 (Fig. 6B). We then asked whether a combination of both Ret-NH_2 and MO treatments impairs 11-*cis*-RAL regeneration upon bright light illumination. To employ this, we subjected RPE65-deficient larvae to Ret-NH_2 treatments but we found no further reduction in 11-*cis*-RAL levels upon illumination (10 000 lux for 20 min) and determination of the 11-*cis*-RAL levels upon 45 min dark-readaption (Fig. 6A). Thus, both MO and/or Ret-NH_2 treatments led to similar reductions in 11-*cis*-RAL levels in the larval eyes. As no additive effects were observed, we concluded that the MO treatment alone efficiently blocked the RPE65-dependent visual cycle. More interestingly, the residual 11-*cis*-RAL was not bleached out under any conditions in repeated experiments (n = 3). This observation indicates that RPE65-independent pathways must exist for the regeneration of the visual chromophore in the zebrafish eyes.

Behavioural consequences of RPE65 deficiency

To directly assess the consequences of RPE65 deficiency on visual performance we employed a vision-dependent behavioural test. This test is based on the optokinetic response that is triggered by movement in the visual field. The ratio of eye movement velocity to the stimulus pattern velocity (gain) is related to stimulus properties such as contrast, brightness, spatial frequency and temporal frequency (Rinner *et al*., 2005b). To compare visual performance between RPE65- deficient larvae and control larvae a contrast sensitivity function was measured; this involved varying the spatial frequency (a measure of stripe width) of a moving grating stimulus. This assay examines visual resolution and contrast sensitivity. Visual performance was not affected in RPE65-deficient morphants as compared to controls under moderate mean luminous intensity (120 cd/m_2; Fig. 7A). In the next experiment we challenged retinoid recycling by measuring contrast sensitivity under dark conditions (0.36 cd/m_2) and with preadaptation to bright light (386 cd/m_2). Contrast sensitivity was indistinguishable for RPE65-deficient and control larvae when measured with a dark grating, while it was slightly reduced under bright light conditions (Fig. 7B). Similar results were obtained by electroretinography (data not shown).

Discussion

RPE65 has been recently identified as encoding the long-sought-after all-*trans* to 11-*cis*-retinoid isomerase in vertebrates (Jin *et al*., 2005; Moiseyev *et al*., 2005; Redmond *et al*., 2005). Here we analysed the role of RPE65 in zebrafish, a species with a cone-dominated retina. For this purpose, we cloned two *RPE65* orthologous genes. We found that only *RPE65a* was expressed during development, spatiotemporally coinciding with the course of photoreceptor development. We disrupted RPE65a by an MO-mediated targeted knockdown to analyse its function in ocular retinoid metabolism. RPE65-deficient larvae possessed significantly reduced levels of 11-*cis*-RAL. Examination of the outer retina in RPE65-deficient larvae by immunohistochemistry revealed unaffected cone morphology and distribution but shortened and deteriorated rod outer segments, while the number and distribution of rods remained unaffected. Thus, RPE65 deficiency interfered with rod photoreceptor function in zebrafish, as has been previously described for *RPE65*$^{-/-}$ mice (Redmond *et al*., 1998).

In contrast to the mouse model (Seeliger *et al*., 2001), RPE65 deficiency did not interfere with cone function. We found sufficient 11-*cis*-RAL to sustain visual performance under bright light conditions. The recent biochemical characterization of RPE65 revealed that its catalytic activity is quite low (Jin *et al*., 2005; Moiseyev *et al*., 2005; Redmond *et al*., 2005). This may explain the large abundance of RPE65, constituting ~10% of total microsomal proteins in bovine RPE (Bavik *et al*., 1992), and the long time course (45 min in mice) for rod visual pigment regeneration upon bleaching (Wenzel *et al*., 2001). Due to these biochemical characteristics of RPE65, we have excluded the possibility that its low residual amounts in the morphants mediate cone function. We have provided further evidence for this assumption by the use of Ret-NH_2, a potent pharmacological inhibitor of the visual cycle (Golczak *et al*., 2005b). In cell culture, we demonstrated that Ret-NH_2 can inhibit RPE65 enzymatic activity. Interestingly, Ret-NH_2 treatments reduced 11-*cis*-RAL levels in control larvae to a similar extent as gene knockdown of RPE65. Most strikingly, Ret-NH_2 had no additive effects in RPE65-deficient larvae, indicating that the MO-treatment alone efficiently blocked the RPE65-dependent visual cycle.

We have thus provided evidence that an additional pathway for 11-*cis*-RAL generation exists in the zebrafish eyes. Our data best fit a model in which visual pigments can be recycled by two independent pathways. One probably represents the established RPE65-dependent visual cycle. In parallel, another retinoid cycle supports cone vision. The existence of this additional pathway is supported by previous data implicating Müller cells in the recycling of the visual chromophore (Goldstein & Wolf, 1973; Hood & Hock, 1973; Saari *et al*., 1982; Bunt-Milam & Saari, 1983; Saari & Bredberg, 1987). Mata *et al*. (2002) have recently provided a model for such a cone-specific pathway that accommodates the elevated demand for 11-*cis*-RAL regeneration under photopic conditions. In contrast to the established visual cycle of rods, this visual cycle probably involves Müller glia cells and depends on a novel type of all-*trans* to 11-*cis*-ROL isomerase (Mata *et al*., 2005). The enzymatic activities of the proposed Müller cell-based pathway could not be detected in retina protein extracts from mice (Mata *et al*., 2002). This difference readily explains that RPE65 gene knockout also affects cone function in this rod-dominated animal (Seeliger *et al*., 2001). However, there is also evidence for all-*trans* to 11-*cis* retinoid isomerases other than RPE65 in mice. Tu *et al*. (2006) have recently reported that melanops-independent photoreception in the inner retina is independent of the RPE65-dependent visual cycle and not susceptible to Ret-NH_2 treatments. Melanopsin resembles in several respects visual pigments of insects, which lack RPE65 (von Lintig *et al*., 2001). Here, both light-dependent and light-independent mechanisms for the production of 11-*cis*-RAL or 11-*cis*-RAL derivatives have been described (Ozaki *et al*., 1993).

The need for the evolution of cone- and rod-specific regeneration mechanisms in animals with high resolution colour vision may have arisen due to a competition for 11-*cis*-RAL between these two types of photoreceptors, which work at different light intensities. This implies that the existence of two visual cycles, an RPE65-based and a possibly Müller cell-based one, might not be limited to cone-dominant species. Humans, for example, have an excess of rods but use cones, particularly in the fovea, for high-resolution colour vision. The observation that children suffering from Leber congenital amaurosis caused by mutations in *RPE65* are able to see colour before losing sight (Lorenz *et al*., 2000; Paunescu *et al*., 2004) supports the existence of an RPE65-independent regeneration pathway for cone visual pigments. The blindness of these patients might be a secondary consequence of the degeneration of rod photoreceptors due to 11-*cis*-RAL deficiency (Woodruff *et al*., 2003) or could result from fragility of cones when unliganded (Rohrer *et al*., 2005; Znoiko *et al*., 2005).

In summary, our study supports the idea of the existence of a conespecific visual cycle. As represented here, the genetic accessibility in conjunction with appropriate techniques establishes the zebrafish as a valuable model for elucidating this pathway in detail.

Acknowledgements

The authors would like to thank Beate Ziser (University of Freiburg) for skilful technical assistance with HPLC analysis. This work was supported by the German Research Council (J.v.L.; DFG LI956-2), the Ministry of Science, Research and the Arts, Baden-Württemberg (J.v.L.), the Swiss National Science Foundation (H.B.S., M.G. and S.C.F.N.), Velux Foundation (S.C.F.N.), the EMBO Young Investigator Program (S.C.F.N.), a ZNZ student fellowship (O.R.), the Roche Research Foundation (O.R.), and ETH internal grants (H.B.S.). S.C.F.N. was an SNF Förderungsprofessor (PP00A-68868). This research was also supported, in part, by NIH grant EY09339 and P30 EY11373. We thank Dr Martin Schwab for helpful comments and financial support. Murine antisera against RPE65 were kindly provided by Dr Andreas Wenzel.

Abbreviations

11-*cis*-RAL
: 11-*cis*-retinal

dpf
: days post-fertilization

hpf
: hours postfertilization

HPLC
: high-performance liquid chromatography

LRAT
: lecithin retinol acyltransferase

MO
: morpholino

RE
: retinyl ester

Ret-NH_2
: all-*trans* retinyl amine

ROL
: retinol

ROS

rod outer segments

RPE

retinal pigment epithelium

RPE65

retinal pigment epithelium-specific 65-kDa protein

References

Bavik CO, Busch C, Eriksson U. Characterization of a plasma retinol-binding protein membrane receptor expressed in the retinal pigment epithelium. J Biol Chem 1992;267:23035–23042. [PubMed: 1331074]

Bernstein PS, Law WC, Rando RR. Biochemical characterization of the retinoid isomerase system of the eye. J Biol Chem 1987;262:16848–16857. [PubMed: 3500173]

Bilotta J, Saszik S, Sutherland SE. Rod contributions to the electroretinogram of the dark-adapted developing zebrafish. Dev Dyn 2001;222:564–570. [PubMed: 11748826]

Bunt-Milam AH, Saari JC. Immunocytochemical localization of two retinoid-binding proteins in vertebrate retina. J Cell Biol 1983;97:703–712. [PubMed: 6350319]

Burns ME, Baylor DA. Activation, deactivation, and adaptation in vertebrate photoreceptor cells. Annu Rev Neurosci 2001;24:779–805. [PubMed: 11520918]

Fan J, Rohrer B, Moiseyev G, Ma JX, Crouch RK. Isorhodopsin rather than rhodopsin mediates rod function in RPE65 knock-out mice. Proc Natl Acad Sci USA 2003;100:13662–13667. [PubMed: 14578454]

Golczak M, Imanishi Y, Kuksa V, Maeda T, Kubota R, Palczewski K. Lecithin: retinol acyltransferase is responsible for amidation of retinylamine, a potent inhibitor of the retinoid cycle. J Biol Chem 2005a; 280:42263–42273. [PubMed: 16216874]

Golczak M, Kuksa V, Maeda T, Moise AR, Palczewski K. Positively charged retinoids are potent and selective inhibitors of the trans-cis isomerization in the retinoid (visual) cycle. Proc Natl Acad Sci USA 2005b;102:8162–8167. [PubMed: 15917330]

Goldstein EB, Wolf BM. Regeneration of the green-rod pigment in the isolated frog retina. Vision Res 1973;13:527–534. [PubMed: 4540349]

Hauptmann G, Gerster T. Two-color whole-mount in situ hybridization to vertebrate and Drosophila embryos. Trends Genet 1994;10:266. [PubMed: 7940754]

Hood DC, Hock PA. Recovery of cone receptor activity in the frog's isolated retina. Vision Res 1973;13:1943–1951. [PubMed: 4542882]

Jin M, Li S, Moghrabi WN, Sun H, Travis GH. Rpe65 is the retinoid isomerase in bovine retinal pigment epithelium. Cell 2005;122:449–459. [PubMed: 16096063]

Kimmel CB, Ballard WW, Kimmel SR, Ullmann B, Schilling TF. Stages of embryonic development of the zebrafish. Dev Dyn 1995;203:253–310. [PubMed: 8589427]

Lamb TD, Pugh EN Jr. Dark adaptation and the retinoid cycle of vision. Prog Retin Eye Res 2004;23:307–380. [PubMed: 15177205]

Lampert JM, Holzschuh J, Hessel S, Driever W, Vogt K, von Lintig J. Provitamin A conversion to retinal via the beta,beta-carotene-15,15′-oxygenase (bcox) is essential for pattern formation and differentiation during zebrafish embryogenesis. Development 2003;130:2173–2186. [PubMed: 12668631]

von Lintig J, Dreher A, Kiefer C, Wernet MF, Vogt K. Analysis of the blind Drosophila mutant ninaB identifies the gene encoding the key enzyme for vitamin A formation in vivo. Proc Natl Acad Sci USA 2001;98:1130–1135. [PubMed: 11158606]

Lorenz B, Gyurus P, Preising M, Bremser D, Gu S, Andrassi M, Gerth C, Gal A. Early-onset severe rod-cone dystrophy in young children with RPE65 mutations. Invest Ophthalmol Vis Sci 2000;41:2735–2742. [PubMed: 10937591]

Mata NL, Radu RA, Clemmons RC, Travis GH. Isomerization and oxidation of vitamin a in cone-dominant retinas: a novel pathway for visual-pigment regeneration in daylight. Neuron 2002;36:69–80. [PubMed: 12367507]

Mata NL, Ruiz A, Radu RA, Bui TV, Travis GH. Chicken retinas contain a retinoid isomerase activity that catalyzes the direct conversion of all-trans- retinol to 11-cis-retinol. Biochemistry 2005;44:11715–11721. [PubMed: 16128572]

McBee JK, Van Hooser JP, Jang GF, Palczewski K. Isomerization of 11-cis-retinoids to all-trans-retinoids in vitro and in vivo. J Biol Chem 2001;276:48483–48493. [PubMed: 11604395]

Moise AR, Golczak M, Imanishi Y, Palczewski K. Topology and membrane association of lecithin: retinol acyltransferase. J Biol Chem 2007;282:2081–2090. [PubMed: 17114808]

Moiseyev G, Chen Y, Takahashi Y, Wu BX, Ma JX. RPE65 is the isomerohydrolase in the retinoid visual cycle. Proc Natl Acad Sci USA 2005;102:12413–12418. [PubMed: 16116091]

Nasevicius A, Ekker SC. Effective targeted gene 'knockdown' in zebrafish. Nat Genet 2000;26:216–220. [PubMed: 11017081]

Ozaki K, Nagatani H, Ozaki M, Tokunaga F. Maturation of major Drosophila rhodopsin, ninaE, requires chromophore 3-hydroxyretinal. Neuron 1993;10:1113–1119. [PubMed: 8318232]

Palczewski K. G protein-coupled receptor rhodopsin. Annu Rev Biochem 2006;75:743–767. [PubMed: 16756510]

Paunescu K, Wabbels B, Wegscheider E, Drexler W, Preising M, Lorenz B. Extending the phenotypical description of patients with early onset severe retinal degeneration (EOSRD) caused by RPE65– mutations. Invest Ophthalmol Vis Sci 2004;45ARVO E-Abstract 4725

Rando RR. Membrane phospholipids and the dark side of vision. J Bioenerg Biomembr 1991;23:133–146. [PubMed: 2010433]

Redmond TM, Yu S, Lee E, Bok D, Hamasaki D, Chen N, Goletz P, Ma JX, Crouch RK, Pfeifer K. Rpe65 is necessary for production of 11-cis-vitamin A in the retinal visual cycle. Nat Genet 1998;20:344–351. [PubMed: 9843205]

Redmond TM, Poliakov E, Yu S, Tsai JY, Lu Z, Gentleman S. Mutation of key residues of RPE65 abolishes its enzymatic role as isomerohydrolase in the visual cycle. Proc Natl Acad Sci USA 2005;102:13658–13663. [PubMed: 16150724]

Rinner O, Makhankov YV, Biehlmaier O, Neuhauss SC. Knockdown of cone-specific kinaseGRK7in larval zebrafish leads to impaired cone response recovery and delayed dark adaptation. Neuron 2005a; 47:231–242. [PubMed: 16039565]

Rinner O, Rick JM, Neuhauss SC. Contrast sensitivity, spatial and temporal tuning of the larval zebrafish optokinetic response. Invest Ophthalmol Vis Sci 2005b;46:137–142. [PubMed: 15623766]

Rodieck, RW. The First Steps in Seeing. Sinauer Associates; Sunderland, Massachussets: 1998.

Rohrer B, Lohr HR, Humphries P, Redmond TM, Seeliger MW, Crouch RK. Cone opsin mislocalization in Rpe65−/− mice: a defect that can be corrected by 11-cis retinal. Invest Ophthalmol Vis Sci 2005;46:3876–3882. [PubMed: 16186377]

Saari JC, Bredberg DL. Photochemistry and stereoselectivity of cellular retinaldehyde-binding protein from bovine retina. J Biol Chem 1987;262:7618–7622. [PubMed: 3584132]

Saari JC, Bredberg L, Garwin GG. Identification of the endogenous retinoids associated with three cellular retinoid-binding proteins from bovine retina and retinal pigment epithelium. J Biol Chem 1982;257:13329–13333. [PubMed: 6292186]

Schmitt EA, Dowling JE. Comparison of topographical patterns of ganglion and photoreceptor cell differentiation in the retina of the zebrafish, Danio rerio. J Comp Neurol 1996;371:222–234. [PubMed: 8835728]

Schonthaler HB, Lampert JM, von Lintig J, Schwarz H, Geisler R, Neuhauss SC. A mutation in the silver gene leads to defects in melanosome biogenesis and alterations in the visual system in the zebrafish mutant fading vision. Dev Biol 2005;284:421–436. [PubMed: 16024012]

Seeliger MW, Grimm C, Stahlberg F, Friedburg C, Jaissle G, Zrenner E, Guo H, Reme CE, Humphries P, Hofmann F, Biel M, Fariss RN, Redmond TM, Wenzel A. New views on RPE65 deficiency: the rod system is the source of vision in a mouse model of Leber congenital amaurosis. Nat Genet 2001;29:70–74. [PubMed: 11528395]

Seiler C, Finger-Baier KC, Rinner O, Makhankov YV, Schwarz H, Neuhauss SC, Nicolson T. Duplicated genes with split functions: independent roles of protocadherin15 orthologues in zebrafish hearing and vision. Development 2005;132:615–623. [PubMed: 15634702]

Solnica-Krezel L, Driever W. Microtubule arrays of the zebrafish yolk cell: organization and function during epiboly. Development 1994;120:2443–2455. [PubMed: 7956824]

Tu DC, Owens LA, Anderson L, Golczak M, Doyle SE, McCall M, Menaker M, Palczewski K, Van Gelder RN. Inner retinal photoreception independent of the visual retinoid cycle. Proc Natl Acad Sci USA 2006;103:10426–10431. [PubMed: 16788071]

Wald G. The molecular basis of visual excitation. Nature 1968;219:800–807. [PubMed: 4876934]

Wenzel A, Oberhauser V, Pugh EN Jr, Lamb TD, Grimm C, Samardzija M, Fahl E, Seeliger MW, Reme CE, von Lintig J. The retinal G protein-coupled receptor (RGR) enhances isomerohydrolase activity independent of light. J Biol Chem 2005;280:29874–29884. [PubMed: 15961402]

Wenzel A, Reme CE, Williams TP, Hafezi F, Grimm C. The Rpe65 Leu450Met variation increases retinal resistance against light-induced degeneration by slowing rhodopsin regeneration. J Neurosci 2001;21:53–58. [PubMed: 11150319]

Westerfield, M. The Zebrafish Book. University of Oregon Press; Oregon: 1994.

Woodruff ML, Wang Z, Chung HY, Redmond TM, Fain GL, Lem J. Spontaneous activity of opsin apoprotein is a cause of Leber congenital amaurosis. Nat Genet 2003;35:158–164. [PubMed: 14517541]

Znoiko SL, Rohrer B, Lu K, Lohr HR, Crouch RK, Ma JX. Downregulation of cone-specific gene expression and degeneration of cone photoreceptors in the Rpe65−/− mouse at early ages. Invest Ophthalmol Vis Sci 2005;46:1473–1479. [PubMed: 15790918]

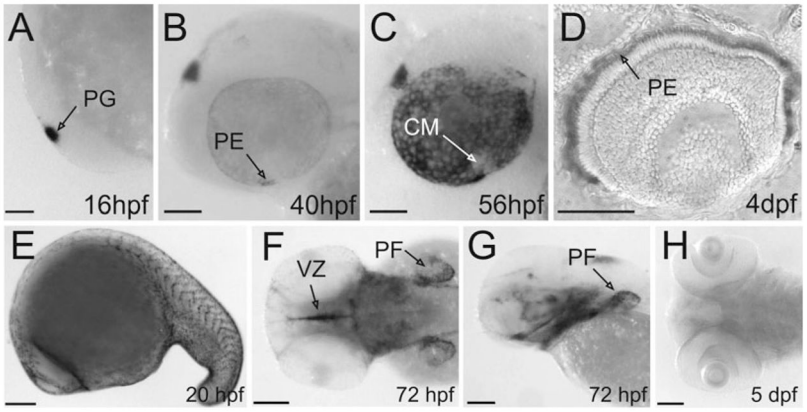

Fig. 1.

Expression of *RPE65a* and *RPE65b* at different developmental stages. (A–C, E and G) Lateral views, anterior toward the left. (D) transverse section through the eyes of 4-dpf larvae. (F and H) Dorsal views, anterior towards the left. (A–D) Expression of *RPE65a*. (A) Beginning at 16 hpf, *RPE65a* was expressed in the pineal gland. (B and C) At 40 hpf, *RPE65a* expression started in the ventral nasal patch of the eyes and spread over the whole RPE at later developmental stages. (D) Transverse section of a 4-dpf larval eye reveals that *RPE65a* expression was confined to the pigment epithelium. (E–H) Expression of *RPE65b*. (E) During segmentation *RPE65b* was expressed in migrating neural crest cells. (F and G) *RPE65b* mRNA was detectable in the developing pectoral fin, the ventricular zone and the upper and lower jaw in early larval stages. (H) *RPE65b* expression faded out in later stages. CM, ciliary margin; PE, pigment epithelium; PF, pectoral fin; PG, pineal gland; VZ, ventricular zone. Scale bars, 100 μm.

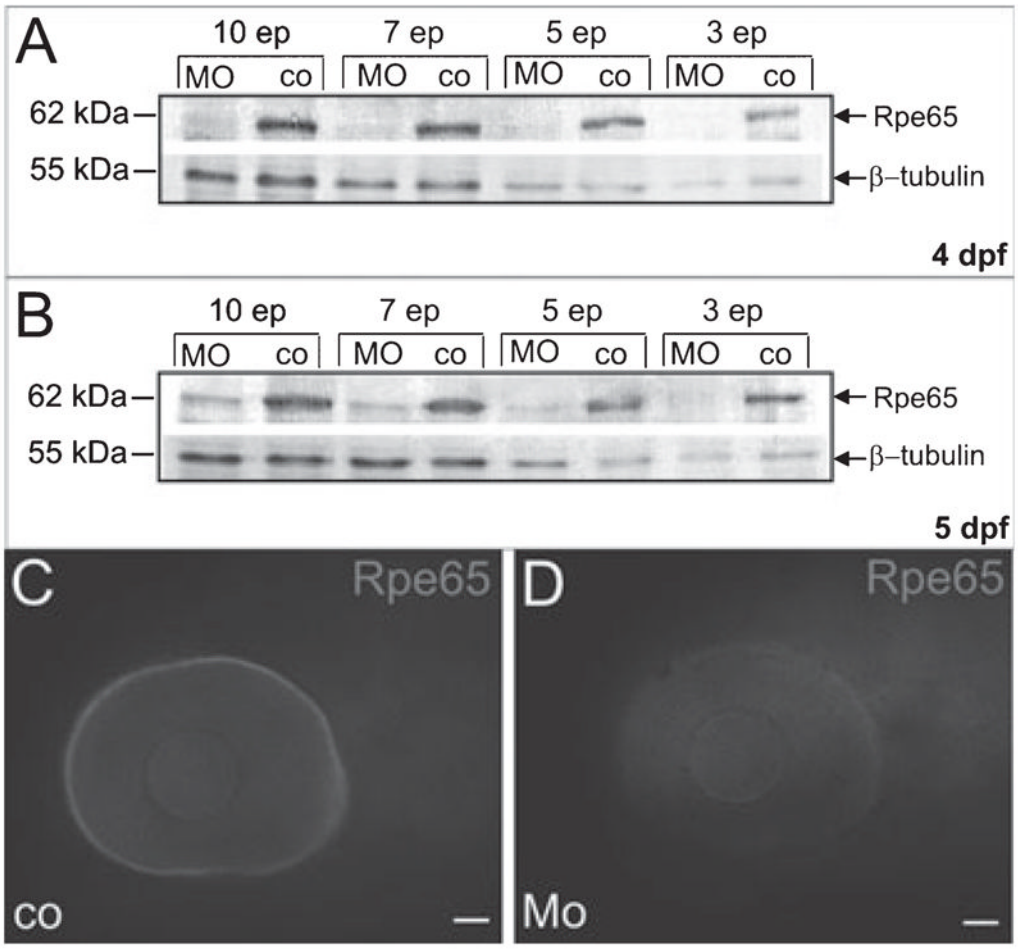

Fig. 2.

MO treatment induced RPE65 deficiency in 5-dpf larvae. (A and B) Immunoblot analysis for RPE65 in protein extracts derived from ten, seven, five and three heads of 4- and 5-dpf *RPE65* morphants and controls; betatubulin was used as a loading control; ep, eye pairs. (C and D) Epifluorescence micrographs of whole-mount immunostainings with an antiserum raised against zebrafish RPE65 confirmed RPE65 deficiency in the eyes of 5-dpf MO-treated larvae. Scale bars, 50 μm.

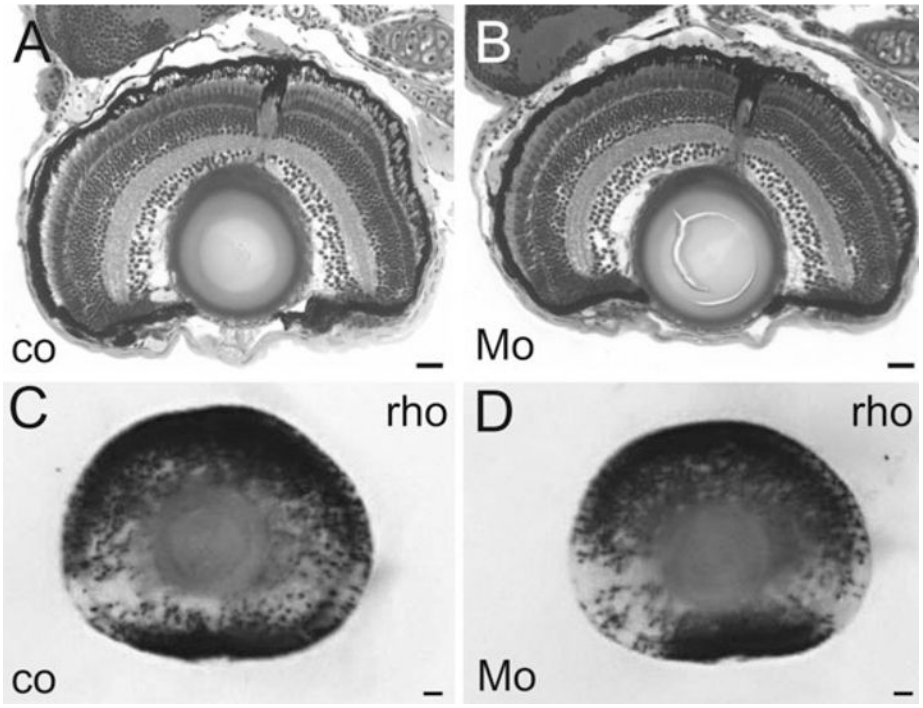

Fig. 3.

Morphology of the eyes of *RPE65a* morphants. (A and B) Transverse sections through the eyes of 6-dpf larvae revealed a normal stratification of the distinct retinal layers. (C and D) Lateral views of the eyes (dorsal on the top, ventral at the bottom, anterior to the left) of 5-dpf larvae stained for rhodopsin mRNA expression. Rods show a similar number and distribution in *RPE65a*-morphant and control embryos. Mo, *RPE65a*-morphant, co, control sibling. Scale bars, 20 μm.

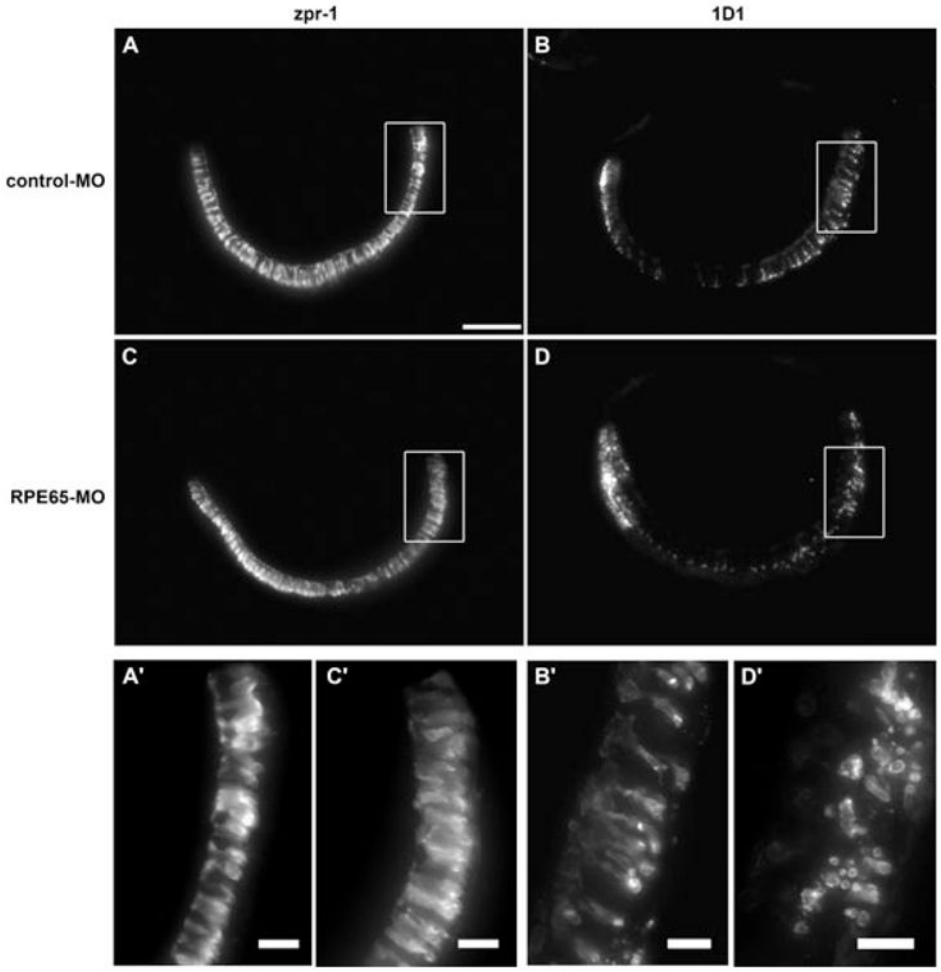

Fig. 4.

Maximal intensity projections of immunostainings for zpr1 (double cones) and 1D1 (rods) in transverse sections of 5-dpf control and *RPE65a*-morphant larvae. (A and C) Zpr1-positive double cones were strongly labelled throughout the entire retina of morphant and control larvae; (A′ and C′) higher magnification of boxed area. (B and D) 1D1-positive rods showed the same distribution pattern in control and morphant retinas. (B′) Higher magnification of the dorsal part of control larva shows normal rod photoreceptor morphology. (D′) RPE65a-deficient larva shows deteriorating rod outer segments breaking up into small particles, presumptive phagosomes. Scale bars, 50 μm (A), 10 μm (A′–D′).

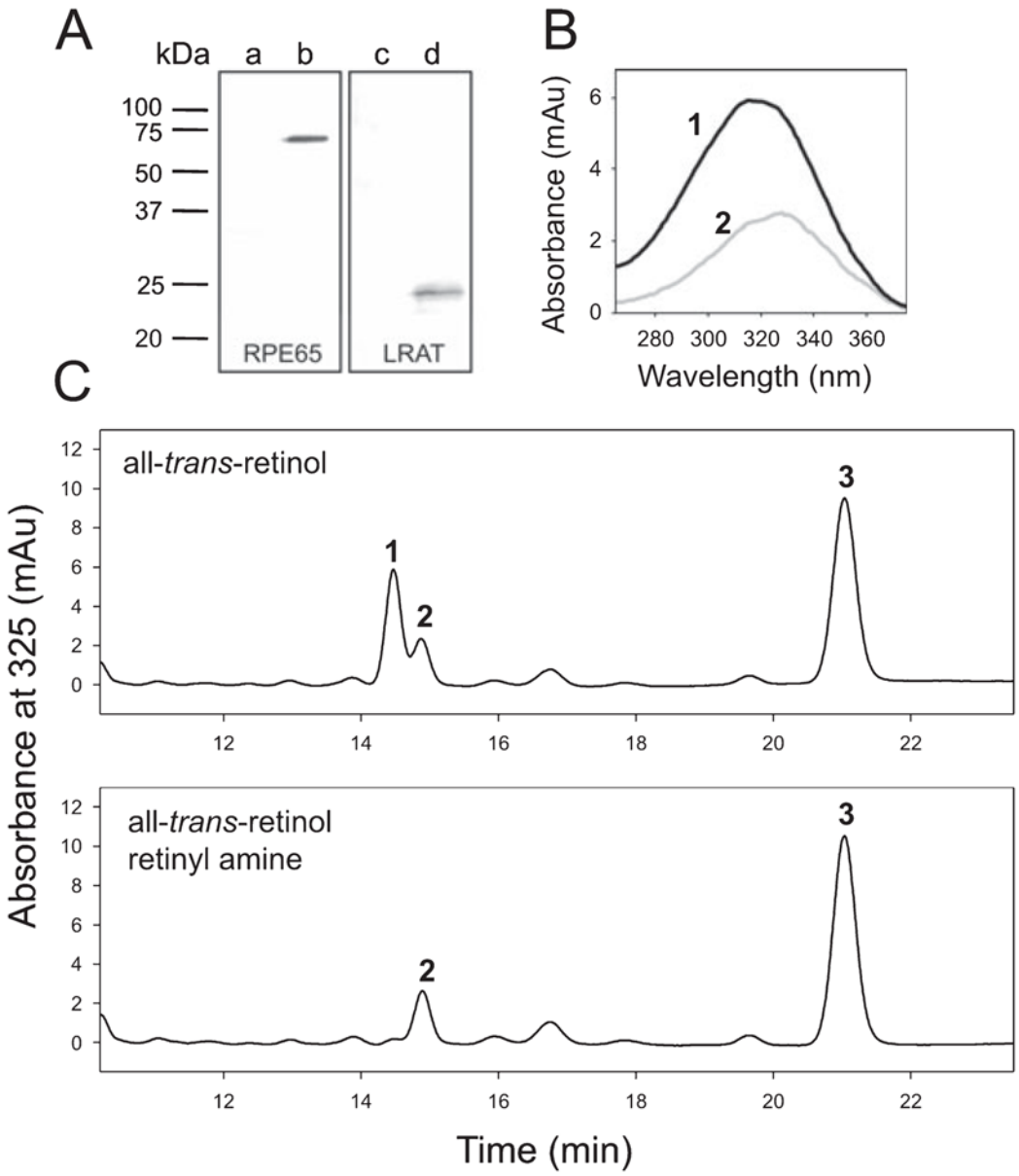

Fig. 5.

Retinylamine inhibited RPE65-dependent isomerization of retinoids. (A) Coexpression of human RPE65 and mouse LRAT inSf9 cells was confirmed by Western blotting. Lines ‘a’ and ‘c’ correspond to uninfected cells while lines ‘b’ and ‘d’ represents cells infected with baculoviruses carrying *RPE65* or *LRAT* cDNA. (B) Absorbance spectra corresponding to peaks 1 and 2 on the chromatograms. Identification of peak 1 as 11-*cis*-ROL and peak 2 as 13-*cis*-ROL was based on elution times, characteristic spectra shapes and absorption maxima at 318 and 328 nm, respectively. (C) Top chromatogram represents retinoid composition extracted from Sf9 cells expressing RPE65 and LRAT incubated with all-*trans*-ROL (10 μM). Robust production of 11-*cis*-ROL was detected (peak 1). Peaks 2 and 3 correspond to 13-*cis* and all-*trans*-ROL, respectively. Addition of all-*trans*-retinyl amine (Ret-NH_2) to a final concentration of 3 mM completely inhibited 11-*cis*-ROL production (bottom chromatogram).

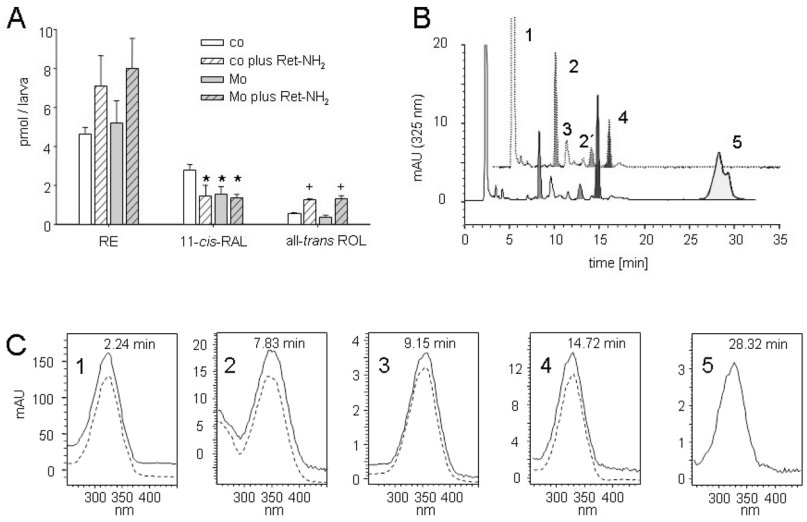

Fig. 6.

Levels of retinoids in 5-dpf larvae subjected to Mo and/or Ret-NH_2 treatment. (A) Retinoid composition of overnight dark-adapted, illuminated (10 000 lux for 20 min) and dark-readapted (45 min) 5-dpf larvae subjected to Mo and/or Ret-NH_2 treatments. The values give the average of three independent experiments for each condition with 75 larvae. $^{*}P < 0.02$ vs. untreated control larvae (Student's *t*-test,); $^{+}P < 0.01$ vs. the corresponding control (Student's *t*-test). (B) HPLC chromatograms of lipophilic extracts of heads of 5-dpf larvae subjected to Ret-NH_2 treatment (lower trace) as compared to untreated controls (upper trace). (C) Spectral characteristics of retinoids (solid lines) from zebrafish larvae as compared to authentic standards (broken lines). 1, RE; 2, 11-*cis*-RAL oxime (syn), 2′, 11-*cis*-RAL oxime (anti); 3, all-*trans*-RAL (syn); 4, all-*trans*-ROL; 5, retinylamide. co, control larva; Mo, *RPE65a*-morphant larva.

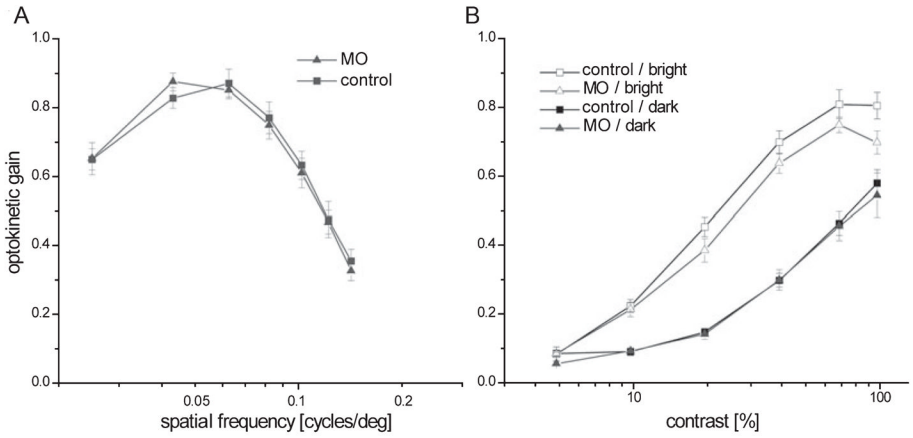

Fig. 7.

Behavioural analysis of RPE65-deficient larvae. (A) Optokinetic gain triggered by moving gratings (velocity 7.5 °/s, contrast 99%) of varying spatial frequency under moderate background intensity (120 cd/m^2) showed no significant reduction in visual acuity in RPE65 morphants (n = 8) compared to controls (n = 8). (B) Optokinetic gain measured with moving gratings (velocity 7.5 deg/s, spatial frequency 0.06 cycles/deg) of varying contrast. Contrast sensitivity of the optokinetic response was not significantly reduced in RPE65-deficient larvae when measured with a dark grating stimulus (n = 5, 0.36 cd/m^2, closed symbols). Under high intensity conditions (n = 5, 386 cd/m^2, open symbols) optokinetic gain was slightly reduced (two-way ANOVA with repeated-measures on factor contrast, $P < 0.05$).

Table 1

Retinoid composition of the eyes of 5-dpf larvae subjected to different light conditions

	RE	11-*cis*-RAL	all-*trans*-RAL	all-*trans*-ROL
Dark				
Control	4.63 ± 0.71	2.82 ± 0.18	0.46 ± 0.03	0.04 ± 0.01
MO	4.5 ± 0.72	1.52 ± 0.08	0.18 ± 0.01	0.08 ± 0.01
Bleached				
Control	6.6 ± 1.19	1.65 ± 0.02	0.34 ± 0.01	0.11 ± 0.01
MO	6.09 ± 1.08	0.53 ± 0.01	0.08 ± 0.01	0.06 ± 0.01
Bleached/dark				
Control	6.28 ± 1.42	2.81 ± 0.18	0.36 ± 0.02	0.01 ± 0.01
MO	5.27 ± 1.14	1.40 ± 0.07	0.40 ± 0.02	0.11 ± 0.01

Retinoids were extracted from 50 larval heads under dim red light and subjected to HPLC analysis. Values (pmol per eye pair) are the mean ± SD of three independent experiments. Dark, dark-adapted overnight; bleached, dark-adapted overnight and illuminated with 10 000 lux for 20 min; bleached/dark, dark-adapted overnight and illuminated with 10 000 lux for 20 min and dark-readapted for 45 min. Control, WT larvae; MO, RPE65a-knockdown larvae.